Acta Astronautica 186 (2021) 269–279

Contents lists available at ScienceDirect

Acta Astronautica

journal homepage: www.elsevier.com/locate/actaastro

Realistic sunshade system at L_1 for global temperature control

Christer Fuglesang *, María García de Herreros Miciano **

KTH Royal Institute of Technology, SE-100 44, Stockholm, Sweden

ARTICLE INFO

Keywords:
Geoengineering
Space sunshade
Solar sail
Global warming

ABSTRACT

So far, space-based geoengineering has rarely been studied from a practical point of view, considered unrealistic as a near-future alternative to fight climate change. This paper evaluates the feasibility of implementing a space sunshade in the vicinity of the first Lagrange point of the Sun-Earth system by the middle of the century. The analysis considers the necessary technological development, the possible trajectories for the shades, and an approximation of the size and cost of the system. It is strongly dependent on the possible optical properties of future solar sails, so an optimal and a more conservative alternative have been studied. With the latter, the shade will be formed by 1.5×10^9 sailcraft with a sail area of 2500 m^2 and a total mass of 8.3×10^{10} kg. In the optimal case, the total mass is 3.4×10^{10} kg. Each one of these sails will be launched to a 2000 km orbit, from where they will travel for about 600 days to the equilibrium point using solar radiation pressure. The total cost of the mission is estimated to be five to ten trillion dollars, based on a launch cost of US$50/kg. There are two main technological challenges for this to become a reality: the low TRL of the solar sails proposed and the necessary development in the launch vehicle industry given the dimensions of the mission.

1. Introduction

The global temperature is increasing and with growing certitude this is due to the emission of Green House Gases (GHG), primarily carbon dioxide (CO_2). Human activities are estimated to have caused approximately 1.0 °C of global warming above pre-industrial levels, with a likely range of 0.8 °C to 1.2 °C [1]. A recent study shows that each decade since 1980 has been successively warmer than the preceding one, and that the 2010–19 decadal temperature departure from average surpassed the previous record warm decade of 2000–09 by 0.15 °C-0.22 °C [2]. It is certain that a too large and too fast temperature increase will have severe social, economic and environmental consequences, and could even be catastrophic to our civilization. Nevertheless, rigorous actions to control the temperature increase will also be costly. The complex relationship between temperature increase and economic and social costs is a difficult and debated topic. Two examples of recent studies are Hänsel et al. "Climate economics support for the UN climate targets" [3] and Hassler et al. "The Consequences of Uncertainty: Climate Sensitivity and Economic Sensitivity to the Climate" [4]. The former conclude that the temperature increase should be limited to a maximum of 2 °C, and preferably 1.5 °C, above pre-industrial values [3], while Hassler et al. show that the uncertainties are very large but conclude that a "laissez faire"-policy is more dangerous than doing too much [4]. The primary course of action is to significantly reduce the emission of CO_2 immediately, and to continue decreasing it until a net zero-emission is reached sometime around the middle of this century [1,5].

There are doubts, however, that the efforts being made today, as well as those planned for the coming decades, to reduce CO_2 emissions will be enough to prevent large damages to the environment, societies and economies [5,6]. It is therefore prudent to look into complementary methods to control the Earth's temperature. Some of these methods are called geoengineering. One way of geoengineering is to limit the amount of sunlight reaching the Earth's surface and thereby limit the temperature increase. This can be done by placing sunshades in space, preferably in the vicinity of the Lagrange point L_1 in the Sun-Earth system. This is a less invasive method compared with other techniques, such as putting aerosols or other reflective particles in the atmosphere, as proposed by many, see e.g. Ref. [7] for a discussion and a recent suggestion in Ref. [8].

The space sunshade concept has been discussed before with various technical solutions [9–17], but it has generally not been considered technologically feasible nor economically realistic. A study by Kosugi in 2010, though, found that space sunshades could be cost-effective and

* Corresponding author.
** Corresponding author.
E-mail addresses: cfug@kth.se (C. Fuglesang), mgdhm@kth.se (M.G. de Herreros Miciano).

https://doi.org/10.1016/j.actaastro.2021.04.035
Received 17 December 2020; Received in revised form 19 April 2021; Accepted 27 April 2021
Available online 29 May 2021

recommended to use them for some hundred years from the latter part of this century [18]. Due to recent technological developments – primarily in the launch vehicles industry, but also by advancements and demonstrations of solar sailing technology [19] – it is becoming reasonable and viable that a space sunshade system could actually be built fairly soon. In contrast to the earlier proposals that assumed in-space manufacturing, we believe that the most realistic way to construct a sunshade system in the near future is to build the shades on Earth and launch them into space. An exception is Angel, who in 2006 [14] suggested a system with small refractive screens manufactured on Earth, but launched with a completely new system based on electromagnetic cannons.

In this article, we will present how a sunshade system could be technically realised and argue that its cost could possibly be much less than the economic damages of not implementing it. Whether it will be economically advantageous or not will to a large extent depend on both the climate and economic sensitivity. In 10–15 years we should have an answer to most of these questions and, in the meantime, it would be wise to spend a limited amount of money on developing and demonstrating the technology required. Thus, humanity could be ready to implement an additional method to prevent global temperature from rising too much, if necessary.

It is too early to say how much shading will be necessary, if at all, but it is likely that a system large enough to reduce the global temperature by the order of 1 °C might be needed. We present a system which would be able to achieve this reduction, but it could easily be scaled in case a larger reduction was required. In a report from 2000, Govindasamy and Caldeira estimated that, to offset completely the effect of doubling the CO_2 content in the atmosphere from the pre-industrial value of 280 ppm–560 ppm, it would be necessary to decrease the incoming solar flux by 1.7% [20]. Without any action, their model gave a temperature increase of 1.75 °C. Another study by Bala, Duffy and Taylor had a similar result, with 1.8% reduction compensating for a doubling of CO_2 content [21]. Based on this, we will size the sunshade system to reduce the sunlight reaching Earth by 1%. For example, this could limit a threatening temperature increase of 3 °C to 2 °C.

The cost of the whole system, we estimate to be several trillion US dollars. However, the cost to society, economy and environment of doing nothing, is probably a couple of orders of magnitude larger, as explained in subsection 8.6.

2. Solar sailing and sunshade system

Solar sailing is a method to accelerate spacecraft without using propellants by using an external force: the Solar Radiation Pressure (SRP). The light particles, the photons, carry a tiny amount of momentum, which transfer a small force to the spacecraft when they bounce, i.e. reflect, on it. In the ideal case, the force is always normal to the surface upon which the photon is reflected and pointing away from the Sun. With a large enough sail in relation to its mass, one can obtain a force that will dominate the movement of the spacecraft. Such a spacecraft will henceforth be referred to as a sailcraft. The direction of the force is controlled by changing the sail attitude in relation to the light flux. For example, as illustrated in Fig. 1, when the sailcraft is orbiting the Sun and the SRP force has a component opposite to the direction of the velocity vector, part of the force will work on reducing this velocity, decreasing its orbital energy, and subsequently the spacecraft will move closer to the Sun.

The force from the sunlight - or indeed from the full electro-magnetic radiation spectrum - on a perfectly reflecting sail, perpendicularly oriented towards the Sun, depends on the sail area A_s and the solar radiation pressure P as

$$F_s = 2A_sP \tag{1}$$

where the factor 2 comes from the fact that the photons effectively make ideal elastic bounces on the sail surface. In reality, there are several corrections to the optical properties of the sail, many of which can be summarized in a "sail efficiency" factor Q. For a specular reflector with Lambertian thermal re-emission, this sail efficiency factor Q is defined as [22,23].

$$Q = \frac{1}{2}\left[\left(1+\eta\right)+\frac{2}{3}\left(1-\eta\right)\frac{\varepsilon_F-\varepsilon_B}{\varepsilon_F+\varepsilon_B}\right] \tag{2}$$

where η is the specular reflectivity, ε_F is the emissivity of the front (Sun facing) side of the sail and ε_B is the emissivity of the rear side. The acceleration from the Sun on a sailcraft with mass m_s then becomes

$$a_s = \frac{2PA_sQ}{m_s}\cos^2\alpha \tag{3}$$

where an arbitrary angle α between the sail's normal vector and the direction to the Sun has been introduced (see Fig. 1). A sail coated with a high-reflective metal could have a $Q \approx 0.9$, while for a non-reflecting black sail with $\eta \approx 0$ and $\varepsilon_F \approx 0$, the sail efficiency could in principle be as low as $Q \approx 0.17$ [24].

An interesting fact is that both the solar radiation pressure (SRP) force and the gravitational force decrease with $\frac{1}{R^2}$, where R is the distance of the sailcraft from the Sun. Their ratio is therefore constant (w.r.t. R), and the acceleration due to the solar radiation can be expressed as a function of the Sun standard gravitational constant, μ_{sun}. By introducing the dimensionless lightness number β, defined as the ratio of SRP acceleration to the solar gravitational acceleration, one can write

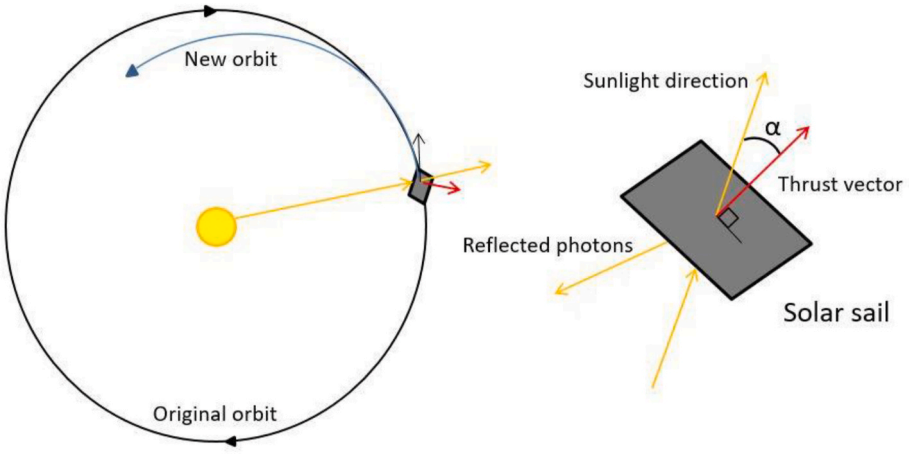

Fig. 1. Solar sail example.

$$a_s = \frac{\beta \mu_{sun}}{R^2}\cos^2\alpha \tag{4}$$

The lightness number β is a function of the sail efficiency Q and the sailcraft areal density ρ_A (also referred to as sail load factor):

$$\rho_A = \frac{m_s}{A_s} \tag{5}$$

The value of β serves as a figure of merit for a sailcraft and with ρ_A in units of g m^{-2}, it becomes

$$\beta = \frac{1.53Q}{\rho_A} \tag{6}$$

The value 1.53 represents the critical loading parameter in g m^{-2}. It is the mass to area ratio that a sail, oriented perpendicular to the sun line, should have to generate a force equal and opposite to the solar gravitational force.

Up to this point, the solar sail has been considered as a flat surface. In reality, though, the thin membrane of the sail will undulate under the radiation pressure, modifying the total force. A force model to simulate this behavior was derived by the Jet Propulsion Laboratory (Eq. (7)), where the total force is parametrized as a function of the angle α between the force of the thrust vector and the sunlight [22]. It must be pointed out that, when using this expression, the force is null for angles larger than 61.1°.

$$F = 2PA_sQ(0.349 + 0.662\cos 2\alpha - 0.011\cos 4\alpha) \tag{7}$$

There is an excellent synergy between sunshades in space and solar sails. Both need to be large and thin, with a mass per area as small as possible in order to reduce the launch cost from Earth, as well as to increase maneuverability in space. However, the total area of the sunshade needed to reduce the solar radiation reaching Earth by 1% is several orders of magnitude larger than the size of any solar sail that can be constructed on Earth and launched to space.

Approximating the Earth with a sphere of radius 6371 km, the cross section area is 1.28×10^8 km^2. Thus, as a first approximation, the total sunshade area has to be at least 1.3×10^6 km^2. Consequently, the full sunshade system under study in this paper was defined as a constellation formed by a large number of much smaller sailcraft. This large group of spacecraft must stay around the equilibrium point with a certain formation in order to form the shadow. To achieve this, a swarm control strategy is proposed, which would allow an autonomous group organization of the sailcraft. This kind of control methods are already being contemplated for reduced groups of observation satellites [25] and could be developed in the following years for larger groups. By using this strategy instead of the randomly placed spacecraft cloud proposed by Angel [14], it is possible to avoid the increase in the number of vehicles needed to compensate for the fraction that could otherwise shade other sailcraft.

A few solar sail demonstration missions have been performed, where the most successful so far have been IKAROS, in 2010 [26,27], and LightSail-2, launched into Low Earth Orbit (LEO) in 2019 [28,29]. The areas of these solar sails were 196 m^2 and 32 m^2 respectively. Several projects studied larger sails, e.g. Sunjammer, with a sail of 1200 m^2 [30], and Heliostorm, with a 10 000 m^2 sail [31], but all of them were cancelled after the design stage.

3. Location of the sunshades

At the Lagrange point L_1 in the Sun-Earth system, the gravitational forces and the centrifugal force of a third body cancel each other. This point is located at 1.5×10^6 km from the Earth, on the line from Earth to the Sun, 1% of the whole distance between the two bodies. A body placed at L_1 will in principle remain there if there are no other external forces, although it is an unstable equilibrium, so in practice it will only stay for a limited time. There are, however, always other external forces present and, for solar sails, the force from the solar radiation pressure (SRP) is the largest one of those. The solar wind is another, but it is almost four orders of magnitude smaller [22]. The SRP force acts in the direction from the Sun and to offset this with increased gravitational pull from the sun, the equilibrium point will move further away from the Earth. How much the displacement of this so called "sub-Lagrangian" point L_1' is depends on the external acceleration of the body, which in turn depends both on the reflectivity and the mass of the body. Higher reflectivity gives a larger SRP force and leads to a larger displacement. A larger mass, on the other hand, "anchors" the body closer to L_1 since the gravitational force becomes larger. Another way to see it is that the acceleration component from the SRP decreases with a higher mass. The exact new location of the point can be calculated by solving the following equation (Eq. (8)), where $\gamma = x_e - (1 - \mu)$, being x_e the distance of the equilibrium point L_1' from the center of mass of the Sun-Earth system along the Sun-Earth line and μ the mass ratio: $\mu = \frac{m_{earth}}{m_{sun}+m_{earth}}$ [16].

$$\gamma^5 - (3-\mu)\gamma^4 + (3-2\mu)\gamma^3 + (1-2\mu-(\beta+1)(1-\mu))\gamma^2 + 2\mu\gamma - \mu = 0 \tag{8}$$

When considering a sunshade, there is one more aspect of interest: The amount of decreased light on the surface of the Earth (ΔS) from a sunshade with a given area, decreases quadratically with the distance from the planet (since the Sun is larger than the Earth), as given by the following expression:

$$\Delta S = \frac{R_{Sun}^2}{R_{Shade}^2}\frac{A_{Shade}}{A_{Sun}} \tag{9}$$

where R is the distance to Earth and A is the cross-section area as seen from Earth.

As seen in (Eq. (8)), the position of L_1' depends on β and thus on the area-to-mass ratio according to (Eq. (5)). Because the required shade area depends on the distance to the Earth as in (Eq. (9)), the position is actually uniquely defined by the mass of the system and the sail efficiency. As a function of the L_1' position, the mass exhibits a minimum at 2.36×10^6 km from Earth (0.9842 AU from the Sun), independent on the sail efficiency Q and ΔS [16,24]. This can be seen in Fig. 2 for a range of Q-values with $\Delta S = 1\%$. At this location the total shade area required to reduce the solar flux by 1% is 3.79×10^{12} m^2. The total mass at the minimum point scales linearly with Q to compensate for the increased solar pressure force with increased gravitational force from the Sun, as shown in Fig. 3.

4. Sailcraft conceptual design

It is clearly preferable to have a low Q in order to minimize the total mass of the whole system. Nonetheless, a high Q is needed to fly the sailcraft more efficiently from Earth to L_1'. We suggest solving this by constructing the sails with two sides with a large difference in

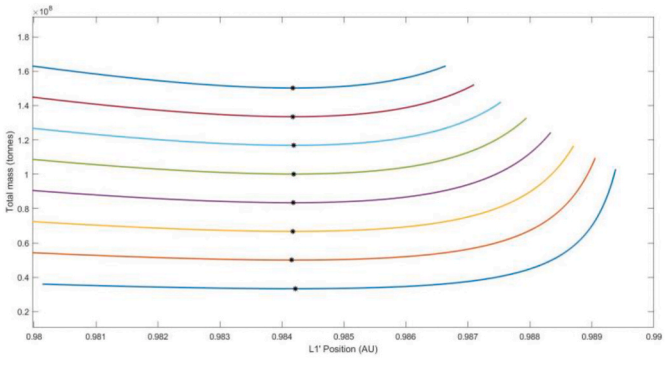

Fig. 2. Minimum mass point location for different values of Q (from 0.2 to 0.9).

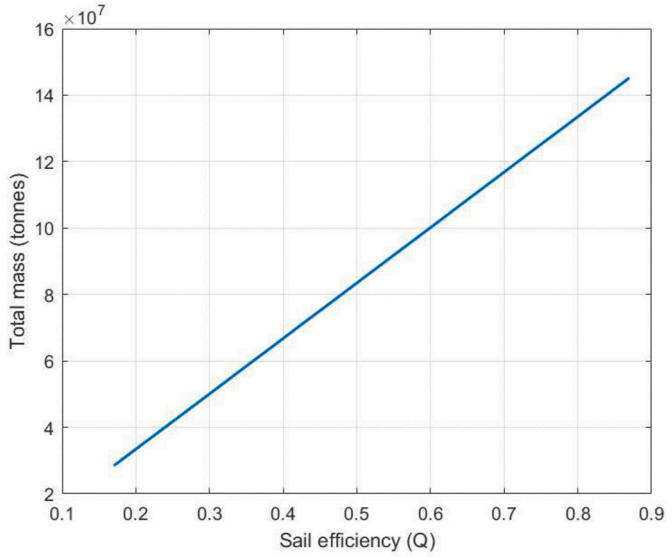

Fig. 3. Variation of the total mass of the system as a function of the sail efficiency.

reflectivity. Although it should be possible to make a sail with an efficiency as high as 0.9, to be conservative the first assumption will be that one side could have $Q = 0.85$ [22], which will be used to get to L_1'. Once there, the sail will be turned around and the other side with a Q as low as possible will face the Sun.

It would be ideal if a sail membrane could be made with a Q as low as 0.2. In practice, this would mean that the side facing the sun would have both very low reflectively and low emissivity, while the other side would have a very high emissivity. Thus, most sunlight would be absorbed, its energy would penetrate through the membrane as heat, and then it would be emitted in the infrared spectrum towards the Earth. Playing with tools like WPTherml [32], it seems that this could be possible. For example, three thin layers (of the order of 100 nm) of TiO_2, Au and Ag (from out-to inside) give a very low reflectivity in the peak of the solar spectrum and almost no emissivity in the infrared. Adding an outer layer with a micro-structure that would let light with optical wavelengths through, while reflecting the longer infrared heat wavelengths, would help to reach values of Q close to 0.2. For example, if both the reflectively η and emissivity on the sun facing side ε_F have values of 0.02 and the emissitvity on the other side $\varepsilon_B = 0.9$, Q becomes 0.2.

A concern could be the temperature T of the membrane. Following the assumptions and method of [22], T is given by

$$T = \left[\frac{1-\eta}{\varepsilon_F + \varepsilon_B} \frac{W_E}{\sigma} \left(\frac{1}{R}\right)^2 \cos\alpha \right]^{\frac{1}{4}} \tag{10}$$

where W_E is the solar constant with a value of 1361 W/m^2, σ is the Stefan–Boltzmann constant and R is the distance of the sailcraft from the sun in AU. In the worst case, with $\alpha = 0$ at $R = 0.98$ AU, the temperature becomes 404 K, which does not pose a problem.

With common materials used currently for solar sailing, though, it is not easy to reach Q values in the low reflectivity side below 0.5. A possible combination that allows reaching this value is black kapton facing the sun and a white paint cover facing the Earth (data from an ESA presentation [33]). These properties result in a Q above 0.9 for the "sailing side" of the membrane, but we will nevertheless stick to $Q = 0.85$ in our calculations. In order to explore the range from what we consider is state-of-the-art today ($Q = 0.5$), to what could ideally be achieved in twenty years ($Q = 0.2$), we have performed calculations for both cases and present the results in this article.

As mentioned previously in section 3, the mass of the system exhibits a minimum at 0.9842 AU and the total mass at this point escalates with the sail efficiency of the sun-facing side. For the two values of Q considered, and a solar flux reduction (ΔS) of 1%, the total mass and corresponding areal density ρ_A (by dividing with the total area of 3.79×10^{12} m) are given in Table 1. Conceptual spacecraft designs were done for sailcraft with areal density 9 g m^{-2} for the ideal case of $Q = 0.2$ and 22 g m^{-2} for $Q = 0.5$.

Based on the literature, the state of the art in solar sailing will allow achieving an areal density of 3 g m^{-2} to 4 g m^{-2} for the sail assembly in 10–15 years [19,34]. We assumed that a value of 4 g m^{-2} could be achievable as explained below. The sail assembly consists of a membrane, four booms and a deployment mechanism. The lightest membrane designed so far was developed by Team Encounter, consisting of 0.9 μm Mylar coated with aluminum on one side and black chromium on the other side, with a resulting density lower than 2 g m^{-2} [35]. The inflatable-rigidizable booms designed in this same project achieved a linear density of 15 g/m [35], adding less than 1 g m^{-2} to assemblies with areas larger than 1600 m^2. Lastly, to approximate the mass that the deployment mechanism and the bonding of the different elements could add, based on other solar sail designs [36], the final areal density of the entire sail assembly was augmented with 1 g m^{-2}.

The control system for the sail angle was not considered as part of the sail assembly, although it might be mounted on the sail. One method to change the attitude of the sail is to adjust the position of center of pressure. To achieve this adjustment, four tip vanes can be mounted in each corner of the sail [37]. The vanes would be able to change their orientation rotating around two axes, independent of each other, allowing active control in any direction. This system will be used as a first assumption for the attitude control, but it will add complexity to the design and deployment of the sail. Its mechanism is accounted for later on in the subsystem mass budget assessment. In the end, this might not be the optimal solution and alternatives are discussed in Sec. 8.1.

As already noted, 4 g m^{-2} of the total density corresponds to the solar sail assembly, leaving the rest for the bus configuration. The spacecraft will need certain subsystems that are almost independent of the sail dimensions (with the exception of the structure, which must be able to carry the solar sail). Once the bus design is settled, the area needed to achieve the selected density can be determined.

Considering the final location selected and the trajectory of the sailcraft, a rough first design of each one of the subsystems was carried out by using as reference the mass of current off-the-shelf traditional space elements for small satellites (some of the companies references are [38,39]). However, the goal of this spacecraft definition was not to achieve a detailed design of the subsystems, but to have an approximate idea of the total mass that the bus could require.

The total mass of the subsystems added up to 35 kg (which corresponds with the bus mass). To this mass, a system margin of 20% was added, considering this very preliminary design [40], resulting in a total mass of 44 kg. For a $Q = 0.2$ and this bus mass, the sail would need to have an area of 8750 m^2 in order to achieve an areal density of 9 g m^{-2}. In case that the optical properties parameter had a value of $Q = 0.5$, the total area would need to be 2444 m^2 to achieve the density of the minimum mass point. The distribution of the mass among all necessary subsystems is depicted in Fig. 4 for both alternatives.

Keeping in mind that the final mass calculated for the bus did not account for harness or any kind of radiation protection, it was decided to raise it to 45 kg. Thus, the area could be defined as 9000 m^2 (with a final mass per sailcraft of 81 kg) or as 2500 m^2 (55 kg per sailcraft) for the two

Table 1
Total mass and areal density of the sunshade system for the two cases under study.

	$Q = 0.2$	$Q = 0.5$
Total mass	3.34×10^{10} kg	8.35×10^{10} kg
Areal density	8.8 g m^{-2}	21.9 g m^{-2}

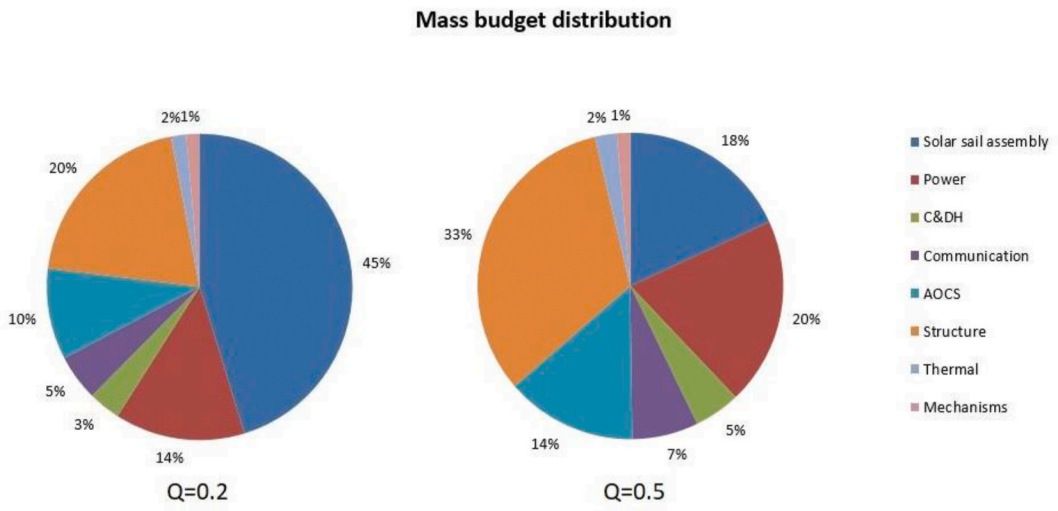

Fig. 4. Mass budget distribution for each subsystem in percentage of the total weight of the sailcraft for both alternatives.

cases. If the final mass per spacecraft gave an areal density lower than the required (9 g m^{-2} or 22 g m^{-2}), it should actually be increased in order to reach the minimum total mass for the shade system. This mass increase could e.g. be used for redundancy of some of the most important elements.

The lifetime for CO_2 in the atmosphere is several centuries, therefore it is important to design a sailcraft with a life as long as possible. At least a 50 years lifetime should be aimed for to keep recurrence cost down (see section 7 below), and therefore each element should be designed or improved for this specific mission requirement. For this reason, even though most of these bus components have a Technology Readiness Level (TRL) of 9, it seemed reasonable to assume a slightly lower TRL given the necessary improvements. These include for example radiation hardness, since the sailcraft will spend an extensive time in the Van Allen radiation belts when escaping Earth, as explained in the next section.

Still, the most important development that must be carried out from a technological point of view involves the solar sail technology [19]. Several sailing projects have reached a TRL of 7 for certain of its subsystems, having completed system demonstration in space environment, such as IKAROS [26,27] and LightSail 2 [28,29]. The TRL of these previous projects was classified as 7 because they aimed to prove some technologies but not to demonstrate solar sailing as a propulsion system. Other sailing technologies have managed to achieve a TRL between 5 and 6. An assessment by NASA after a 20-m ground test in 2006 concluded that TRL was between 3 and 6, depending on the subsystem [41]. A more recent qualification was done in 2016 within the DLR-ESA GOSSAMER project, reaching a TRL of 5 [42], but for a sail of 25 m^2, much smaller than what is considered here, although they later aim for considerably larger sails. A reasonable estimate for the TRL for a sailcraft as envisioned here, with a sail area between 2500 m^2 and 9000 m^2, is between 3 and 4.

5. Getting to L_1′

The journey for a sunshade sailcraft to L_1' will start by launching it on a rocket from a place close to the Equator on Earth. A vehicle launching from the Equator can take considerably more payload to a low-inclination orbit than one launching from a higher latitude, by utilizing the rotational speed of the Earth. The sailcraft will be put in an orbit with an altitude of 2000 km, which is the very top of the so called Low Earth Orbit (LEO) region, and well above the altitude were atmospheric drag still has a small influence (up to 900 km [43]). This altitude was selected also because it will be above the super-constellations of satellites planned for the next years (e.g. Starlink [44] and OneWeb [45]), which are mainly in the range of 500–1500 km. The escape time from Earth is less for higher altitudes, but, at the same time, less payload can be delivered there by a given launcher.

Once in orbit, the sailcraft will deploy its sail and the solar sailing starts. The trajectory was divided in two different phases: the escape trajectory, where the sail leaves the gravitational field of the Earth, and the travel to the equilibrium point L_1'. For all trajectory calculations the circular restricted three-body problem equations of motion were used. In these equations, a Circular Restricted 3-Body (CR3B) reference frame is employed, with the origin at the center of mass of the Sun-Earth-sailcraft system. The x-axis of the right-handed orthogonal system is along the Sun-Earth line towards Earth and the z-axis is perpendicular to the ecliptic plane. The y-axis is approximately parallel to Earth's motion around the Sun (see Fig. 5). It is common to use the unit of mass as the sum of the masses $m_{sun} + m_{earth} = 1$, the unit of length as the distance between the Sun and the Earth (1 AU) and the time unit as $\frac{1}{\omega}$, where ω is the angular velocity of the Earth around the Sun. In this reference frame and with the units mentioned, the motion of the sailcraft can be described as:

$$\ddot{\vec{r}} + 2\vec{\omega} \times \dot{\vec{r}} = \vec{a}_s - \nabla U \tag{11}$$

where U represents the effective gravitational potential, which can be written as:

$$U = -\frac{x^2 + y^2}{2} - \left(\frac{1-\mu}{|\vec{r}_1|} + \frac{\mu}{|\vec{r}_2|}\right) \tag{12}$$

The position vectors $\vec{r}_1$ and $\vec{r}_2$ are defined as $\vec{r}_1 = [x+\mu \quad y \quad z]$ and $\vec{r}_2 = [x-(1-\mu) \quad y \quad z]$ and μ is the mass ratio as in Eg. 8. With these dimensionless units and denoting unit vectors with "hat"($\hat{}$), the SRP acceleration becomes

$$\vec{a}_s = \beta \frac{1-\mu}{(\vec{r}_1)^2}(\hat{r}_1 \cdot \hat{n})^2 \hat{n} = \beta \frac{1-\mu}{r_1^2}\cos^2\alpha \hat{n} \tag{13}$$

with α as defined in section 2 and shown in Fig. 1.

For the first trajectory part, to escape from the Earth orbit, the instantaneous rate of increase of the specific orbital energy was maximized, achieving a near minimum time trajectory [46]. As a consequence, the component of the SRP acceleration along the velocity vector $\vec{v}$ must be maximized in each point by rotating the sail. The specific orbital energy is defined as:

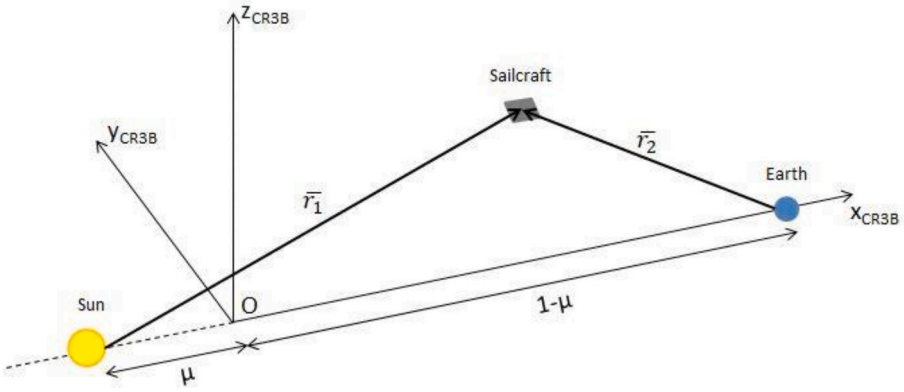

Fig. 5. Three Body Problem reference frame.

$$E_{orb} = \frac{1}{2}\vec{v}^{T}\vec{v} - \frac{\mu_{Earth}}{r} \quad (14)$$

where μ_{Earth} is the Earth's standard gravitational constant and r represents the distance between the Earth's center and the sailcraft. When the specific energy becomes positive, it is considered that the sailcraft has entered a hyperbolic trajectory and therefore can escape Earth. The technique used here follows Coverstone and Prussing [46], but with the additional simplification that the orbit of the Earth around the Sun was considered circular.

The complete trajectory analysis presented is the one corresponding to the sail membrane alternative considered most realistic ($Q = 0.5$), which resulted in an optimal areal density of 22 g m^{-2}. Using a sail efficiency of $Q = 0.85$ on the high reflectivity side, the resulting lightness number $\beta = 0.0591$. With this value and taking the sail force model of Eq. (7) into consideration, the resulting escape time is around 350 days. The exact value depends on the time of the year when the maneuver starts, due to the Earth's orbital inclination with respect to the solar ecliptic plane.

During the Earth escape it is assumed that the sail can be optimally oriented at every instance, which poses strong requirements on the control system. Since the sail force model of Jet Propulsion Laboratory (Eq. (7)) is used, the sailcraft will only increase its orbital energy when the sun angle is between $-61°$ and $+61°$. During the remainder of an orbit, the sail must rotate back by $122°$ to $-61°$ (see Ch. 4.4 in Ref. [22], but where an ideal sail is assumed and therefore an immediate $180°$ rotation is made). At the starting orbit of altitude 2000 km, the time for this is around 40 min, however 32 min of that would be in the shade. It might not be possible to design a control system based on vanes capable of achieving these changes and some alternatives are discussed in section 8.1.

Once E_{orb} has become positive, the travel to the equilibrium point L_1' starts. To solve the optimal control problem of how to orient the sail over time in order to reach the goal in the minimum time possible, the so called "direct method" was used. This method divides the whole flight in segments with constant sail attitude in each one of them, transforming the optimal control problem into a parameter optimization. As shown by Otten and McInnes [47], this nevertheless provides a near-minimum time trajectory. Twenty segments were used and the time was minimized by varying the two angles that define the sail attitude per segment, i.e. in total forty parameters. The SNOPT optimization software, which uses a sequential quadratic programming (SQP) algorithm, was used in MATLAB [48] to find the minimum value numerically.

The final requirement set was that the velocity when arriving at L_1' must be maximum 10^{-4} in dimensionless units (around 3 m s^{-1}) in each coordinate direction. As previously stated, the exact numbers for the final trajectory will change slightly depending on the time of the year when the mission starts. Considering the start of the trajectory at the winter solstice, the flight time from leaving Earth's direct influence ($E_{orb} = 0$) to L_1' with the method above became 747 days, giving a total travel time of 1096 days.

A disadvantage with this initial approach is that the sailcraft always leaves the Earth's influence with a velocity in the direction opposite to the Sun. This fact is not beneficial for the next trajectory phase, which requires moving towards the Sun and not away from it, and therefore, adds up a considerable amount of time to the final solution. Even though the travel time is not critical, since a trajectory of several years can be assumed when compared with the total length of the mission, a search for an alternative trajectory was carried out in order to reduce the final time.

Given the complexity of unifying both phases in one and optimizing the trajectory as a whole, the two-phase division was maintained but a modification was done in the first phase approach. The near minimum time strategy was applied to the escape trajectory until the energy reached a certain pre-set negative value, before reaching a null orbital energy. Here, the control strategy was changed to maximize the acceleration in the direction of the velocity only when this velocity had a component that was directed towards the Sun. A study for different energy values was carried out looking for the optimal exit conditions, considering as such a velocity directed towards the sun combined with a low increase in the escape time with respect the first optimization.

With the second strategy presented and using as a pre-set energy value of -2.94×10^5 J kg^{-1} (about 1% of the initial value of -2.38×10^7 J kg^{-1}) to change the strategy, we found an escape time of 531 days and a total travel time of 603 days. Table 2 summarizes the values for the times and positions in the critical points of this new strategy. The whole trajectory is shown in Fig. 6 and the control history for the second phase can be found in Fig. 7.

If the optical properties of the sailcraft would allow to reach $Q = 0.2$, these numbers would be reduced, since the lightness parameter would have a value of $\beta = 0.145$ and therefore the efficiency of the sail would

Table 2
Key points in the trajectory from LEO to L_1' with Q = 0.5.

	Initial position LEO	Earth escape point	L_1'
Days to reach the point	0	531	603
Position ECI[a] (km)	[8.38 0 0] × 10^3	[115 147 50] × 10^4	[-1.9 −1.2 0.6] × 10^6
Velocity ECI[a] (m s^{-1})	[0 6.9 0] × 10^3	[−80 472 428]	[-277 -348 -155]
Position CR3B (km)	[150, −0.0084 0] × 10^6	[148 0.68–0.13] × 10^6	[147 0 0] × 10^6
Velocity CR3B (m s^{-1})	[6.32 0–2.75] × 10^3	[−423 116–204]	[2.98 2.98 2.98]

[a] Earth-Centered Inertial reference frame.

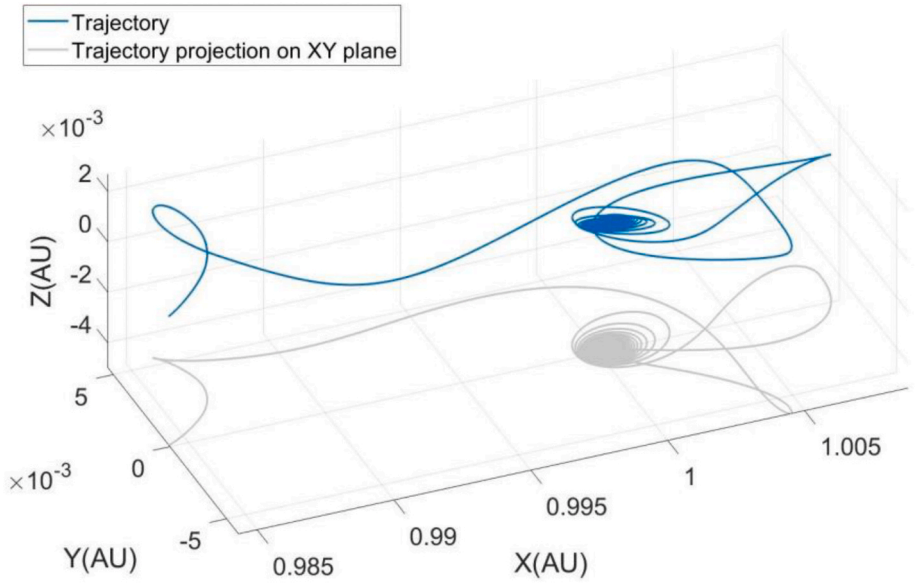

Fig. 6. Final trajectory of the sailcraft from LEO to L_1' and trajectory projection on the XY plane. Note difference in scale of X vs. Y and Z.

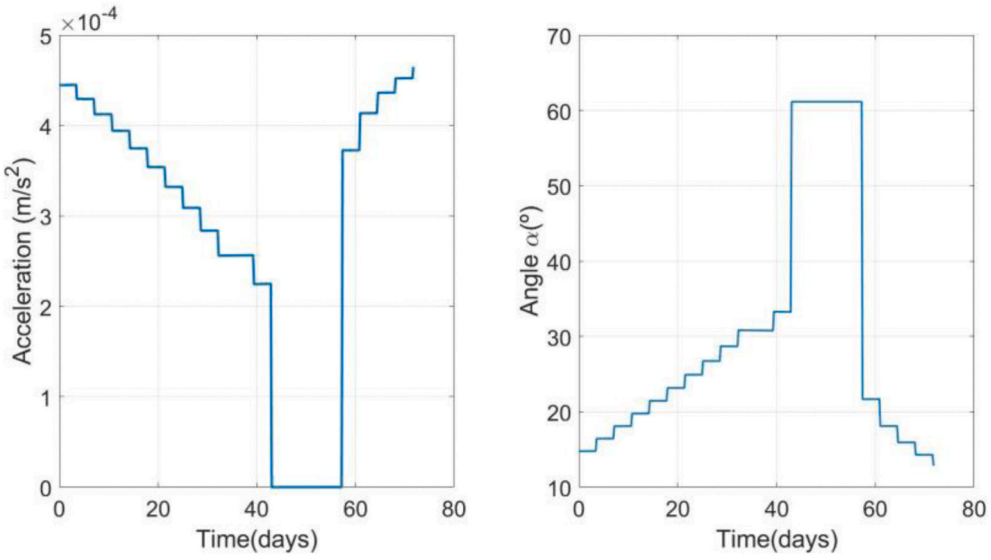

Fig. 7. Magnitude of the acceleration (left) and the angle between the sunlight and the normal to the surface (right) along the second phase of the trajectory. The angle was limited to 61.15° because for angles above this value the force is null (Eq. (7)).

be higher. With the first strategy used, the escape time would result in 190 days, with a final time to reach L_1' of 554 days. Using the second strategy described previously, with a pre-set value for the energy of -3.54×10^5 J kg^{-1}, the escape time would be 285 days, with a total trajectory time of 373 days. The summary of the most important points and times in this case can be found in Table 3.

The final destination of the sailcraft, L_1', corresponds with the equilibrium point for sail membrane side with the lower value for Q, but, as explained previously, in order to achieve a more efficient transfer, the other side with a value set to $Q = 0.85$ was used for the trajectory phase. This means that, once L_1' has been reached, the sail will need to change its orientation 180° in order to face the Sun with the side that was previously in the shadow. This process could take some time and cause a certain drift in the position, which would have to be corrected for afterwards.

As soon as the low-Q side of the sail is facing the sun, the station-keeping strategy will start, in order to keep the sail in the desired

Table 3
Key points in the trajectory from LEO to L_1' with Q = 0.2.

	Initial position LEO	Earth escape point	L_1'
Days to reach the point	0	285	373
Position ECI[a] (km)	[8.38 0 0] × 10^3	[4.82–1.52 3.17] × 10^4	[0.30–2.12 −0.92] × 10^6
Velocity ECI[a] (m s^{-1})	[0 6.9 0] × 10^3	[−1.97 3.06 0.37] × 10^3	[457 56 28]
Position CR3B (km)	[150, −0.0084 0] × 10^6	[150–0.010 0.035] × 10^6	[147 0 0] × 10^6
Velocity CR3B (m s^{-1})	[6.32 0–2.75] × 10^3	[−1.38 3.26–0.88] × 10^3	[2.98 2.98 2.98]

[a] Earth-Centered Inertial reference frame.

position. The precise strategy will depend upon what will be considered optimal at the time. It could be using a natural orbit around L_1' [49] or it could be to have the sunshades follow a trajectory that would give an optimal latitude-dependence of the shade effect, as proposed by Sanchez and McInnes [16].

6. Schedule

A single sailcraft as designed above has a sail area of 9000 m^2 and a mass of 81 kg in the optimal case and 2500 m^2 and 55 kg in the more conservative case. In both options, though, the sailcraft will be positioned at a sub-Lagrangian point L_1' at 2.36 × 10^6 km from the Earth (0.9842 AU from the Sun). The total area required there to reduce the sunlight on Earth by 1% is 3.79 × 10^{12} m^2. Thus, 4.2 × 10^8 sailcraft would be needed in the first case and 1.5 × 10^9 sailcraft for $Q = 0.5$. Assuming a launch vehicle similar to the Starship Super Heavy [50], currently under development with a payload capacity of 100 000 kg to LEO, a total of 330 000–830 000 launches would be required. (The environmental impact of these is discussed in Sect. 8.5.) Considering that the sunshade system might need to be in place by the middle of the century, and that the development required for some of the technologies will need at least 10 years, it was decided to consider a 20 years period for the whole system to be put in space. These figures would mean launching an average of 46 rockets a day (16 700 per year) in the optimal case ($Q = 0.2$) and 114 a day (41 500 per year) in the case of $Q = 0.5$. These are numbers well above the current rate of about 100 launches per year. However, space industry and space flights are slowly becoming more routine and compared to the 45 000 daily flights handled by the Federal Aviation Administration [51], something like one hundred seems like a small number. It will be required to build several new space ports, though. Perhaps six launches per day could be accomplished per launch site, in which case, up to twenty space ports would be needed.

7. Cost of the system

There are two main contributions to the total cost for such a sunshade system: manufacturing and launch from the surface of the Earth to the initial orbit of 2000 km altitude. Today, in 2020, the lowest cost for launching a mass to LEO is about US$2000/kg, compared to the old "rule-of-thumb" which was US$10 000/kg. The price has fallen mainly due to the introduction of reusable rocket stages, being the leading company SpaceX that currently advertises on the website a price of US $90 M for a Falcon Heavy launch, which can take up to 63 800 kg to LEO [52]. The technology of reusability is continuously progressing and, in about a decade, there will likely be completely reusable launch vehicles. SpaceX is well ahead in the development of their Starship and Super Heavy launch systems, which will be fully reusable and able to take 100 000 kg to LEO [50]. The CEO, Elon Musk, has claimed in an interview [53] that the cost for a single launch eventually could be as little as US$2 M, slightly more than twice the cost of the propellant only (methane and liquid oxygen). That would correspond to as little as US $20/kg in launch cost to LEO. On the one hand, we consider this perhaps too optimistic, but on the other hand, a launch system for millions of identical sailcraft could possibly be optimized specifically for this purpose, leading to a low cost. In this case, Starship with Super Heavy would only be showing what realistically could be achieved. Nevertheless, we will make a conservative estimate, assuming a launch cost of US$50/kg for the sunshade system. This also takes into account that prices for launching to LEO normally assume a polar orbit at 500 km altitude, while we need to go to 2000 km, albeit to an equatorial orbit. Thus, the total launch cost for launching all sailcraft with a total mass of 3.4 × 10^{10} kg to 8.3 × 10^{10} kg is estimated to be around US$1.7 × 10^{12} to US$4.2 × 10^{12}.

The results show numbers never seen before in the space industry. Although some large communication constellations are being planned, such as SpaceX Starlink with around 12 000 satellites [54], this figure is around 30 000 times smaller than the number of sailcraft needed. Consequently, the manufacturing cost approximation could not be based on previous spacecraft production experience and, in order to estimate this cost, a comparison with the car industry was made. The sailcraft will be mass produced, like popular car models. The manufacturing cost of a normal car is about US$10 000. However, the sailcraft will likely be less complex than a car and only a tenth in mass. Cost can often be assumed to scale with mass, and it is therefore reasonable to assume a cost of the order of US$1000 per sailcraft. Nevertheless, considering all the uncertainties and to be conservative, this value was doubled and the final estimate for the manufacturing cost was set to be between US$8 × 10^{11} and US$2 × 10^{12}.

There will be additional costs, such as for development, constructing launch sites and manufacturing launch vehicles. They should all be smaller than the values given above, but rounding up to a total cost for everything, we estimate the final values to be the ones represented in Table 4, or to be less precise: "a few trillion" dollars.

These costs will be spread over at least 20 years, so the deployment cost of the initial sunshade system will be in the range US$150 to US $350 billion per year. It could involve many countries, which could each make various contributions, from manufacturing to launch and operations, thus strengthening their industries. This will facilitate finding a political solution for financing. If such a system is needed, it will however likely be required for several centuries, since emitted CO_2 stays in the atmosphere for several hundred years and possibly even up to 1000 years [55]. Assuming an average lifetime of the sailcraft to be 50 years, the replacement cost will be about US$100 billion per year, from the end of the current century. It can be noted that the Voyager spacecraft are still operating after 43 years in space [56].

8. Discussion

8.1. Assumptions made during the study

This paper addresses the practical feasibility of implementing a space sunshade system near the first Lagrangian point and estimates a cost for it. During the study, several assumptions and simplifications have been done by necessity, some of the more critical ones are discussed below.

(i) Solar sail membrane. Although the model selected for the solar radiation pressure force accounts for optical and physical imperfections of the sail, the tangential force component was ignored, considering just a force in the direction of the normal to the surface. Another factor that was not considered is the degradation of the membrane due to solar radiation, particle radiation and micrometeorites, which will also change the value of Q [57].

We have assumed a lifetime of 50 years, but if such a long life was not possible the maintenance cost per year would increase.

It seems plausible that a sail membrane with a "sail efficiency" Q of 0.5 can be manufactured, but it should also have a low areal density, which has here been assumed to be 3 g m^{-2}. A larger areal density of the membrane could be handled by increasing the area of the sail, keeping

Table 4
Cost calculation summary.

	Cost (US$) per kg	Total cost $Q = 0.2$ (US$)	Total cost $Q = 0.5$ (US$)
Launch	50	1.7 × 10^{12}	4.2 × 10^{12}
Spacecraft manufacturing	25	8 × 10^{11}	2.1 × 10^{12}
Additional costs	–	5 × 10^{11}	5 × 10^{11}
Final cost of the whole system	75	3 × 10^{12}	7 × 10^{12}

the same overall areal density of the sailcraft and total mass of the system. Although a smaller sail would easier to design, with 6 g m^{-2} and all other parameters the same, the sail area needed would be 3000 m^2 which is only 20% larger.

A final point is that it could be difficult to achieve a high Q on one side and a low on the other side. It is, though, not so important to have a high sail efficiency. For example, with $Q = 0.7$, the travel time increases only around 20% compared to $Q = 0.85$.

(ii) Attitude control and solar sail structure. Assumptions have been made based on preliminary designs and tests of much smaller systems than here foreseen [35]. We estimate that today the TRL for a 9000 m^2 sail is around 3. Perhaps a TRL of 9 will not be feasible in even 15 years and the system will need to be more massive, which would scale the costs proportionally. The attitude control system must, for example, be sufficiently robust to turn the sail in synchronization with the sailcraft's orbit around Earth, which has an orbit time of just over 2 h at 2000 km (and then decreasing when the sailcraft's mean altitude increases). A minor related simplification made was that the change between different angles for the second phase of the trajectory was considered to be instantaneous. This could to some extent affect the times calculated, increasing the final results, but it would likely be negligible.

There are several possible ways to ease the particular challenge given by an initial launch to 2000 km altitude. The simplest would of course be to chose a higher altitude, but in order to keep launch costs down we decided to explore other methods. Increasing the capabilities of the sail's attitude control system by, for example, having a small electrical motor in addition to the control vanes could be one possibility. Another is to use a small electrical propulsion system that could work in parallel with the solar sail in the initial phase. There are already some on the market having an ISP up to 6000 s [58]. The mass of the propellant needed to raise the Orbit from 2000 km to 10 000 km using this type of propulsion would be less than 2 kg. One could also consider letting the sail continue to rotate in one direction and on every second orbit have the low-reflectively side face the sun. The requirement on the attitude control authority will be much less in this case, while if this is done without any other measure the escape time for the sailcraft will increase about 20%.

(iii) Trajectory time. A strategy was found which showed that the travel time from launch to the desired L_1' point could be kept to about 600 days. This was, though, not an absolute optimization since the time is not a critical factor in the mission. It is likely that the travel time can be decreased through further studies.

8.2. Technology development needed

The low TRL of the main technology required for the project in hand, a large solar sail with specific sail efficiencies (Q) for each side, means that a considerable amount of money will be needed for research and development. Nonetheless, even if in the end the sunshade system is not implemented, the development of this kind of technology will be useful for the space sector in the future. Some of the applications that solar sailing could have include: deorbiting of satellites, acting as main propulsion system of deep space or interplanetary missions, and enabling new non-Keplerian orbits [59,60].

8.3. Climate effect latitude dependence

This research did not carry out a climate analysis of the effects that the shade would have on Earth if implemented, but other studies regarding these consequences have been performed. Lunt et al. [61] were the first to use a fully coupled General Circulation Model to study regional effects of a uniform reduction of the radiation. They found different effects depending on the latitude, achieving significant cooling on the tropics and a warming on high latitudes, even though the global mean temperature decreased. Nevertheless, they concluded that, although these regional differences would exist in the geoengineering world, they would be small when compared with alternative scenarios with high CO_2 emissions and no further actions. Later on, other studies have considered a non-uniform reduction in order to decrease these regional effects [16,62]. As shown by Sanchez and McInnes [16], this can be achieved by making sunshades move in certain orbits around the optimal L_1'. To obtain an ideal differentiation of shading, it might however be necessary to increase the total area, and thus the mass, perhaps as much as 50% with respect to the values given in this paper.

8.4. Collision risk in orbit

By choosing 2000 km as starting altitude, the high density of satellites and space debris in LEO is avoided, but the solar sail will need to face the GEO area. The large dimensions of the sail surface increase the possibility of it being damaged by space debris or micrometeoroids, which would limit the performance of the vehicle. The sailcraft orbit should actually get a small inclination, which will not reflect much in launch cost or in time if done by SRP in the early solar sail phase, and thereby have much lower collision risk with GEO (Geosynchronous Equatorial Orbit) satellites. In addition, about 200 000 sailcraft will be launched per day and it will probably be necessary to put them in slightly different orbits. Since the sailcraft are not foreseen to have any propulsion system, they will not be able to maneuver themselves quickly out of the way for other satellites, so careful planning will be needed. If these issues turn out to be too complex to solve, either starting in a higher orbit or adding a propulsion system should not be excluded, although it would increase considerably the total cost of all launches.

8.5. Environmental impact

An environmental impact assessment was considered necessary to evaluate the implementation of the system, given the final goal of the project. If the development of the system had considerable negative effects on the climate, it would be counteracting its own objective. To account for these effects, the environmental impact is considered to come from three main sources: the launches, the fuel production and the manufacturing of the system.

The impact of the launches comes from emissions from the combustion process. These emissions will depend on the fuel used. Studies regarding rocket emissions are few and not thorough; hence the consequences of these are quite uncertain. Still, from an environmental point of view, the use of rockets powered by liquid hydrogen (LH_2) and liquid oxygen (LOX), which only produces water exhaust, seems to be the best option. Even though, it must be kept in mind that high concentrations of water vapor emissions will also have an effect on the atmosphere that must be studied.

However, LH_2 powered rockets do not seem to be present in the ongoing development of heavy launchers. The vehicle considered above to launch the sailcraft was the Starship, which runs with methane (CH_4) and LOX, giving as main products of the combustion CO_2 and H_2O. Table 5 shows approximations of the amount of CO_2 emissions (considering a perfect combustion of the reactants) in the worst case

Table 5
Carbon dioxide emissions calculations for Starship launches (Q=0.5 case).

Total propellant mass per launch	4500 tonnes
Methane mass per launch	900 tonnes
Carbon dioxide emission per launch	2475 tonnes
Carbon dioxide emission in one year	102 million tonnes
Total carbon dioxide emissions	2054 million tonnes

scenario, which corresponds with the $Q = 0.5$ alternative. The total number of annual emissions represents only 11% of the emissions from commercial aviation in 2019 [63] and 1.2% of the ones from passenger cars in 2018 [64]. Furthermore, when considering the current amount of CO_2 in the atmosphere [65], the emissions of this project represent around 0.2%. These comparisons lead us to think that, even if the launch vehicle used has a certain contribution to the CO_2 emissions, the magnitude of this amount could be accepted given the later benefits of the mission.

The sustainability of the rocket fuel production shows similar outcomes for both of the fuels mentioned above. Carbon neutral fuels could be obtained using exclusively renewable energy, which would allow the production process to stay carbon neutral as well. Meanwhile, although methane is abundant on Earth and could be obtained as a fossil fuel, it can also be produced by an electrolysis process using CO_2 and water, which can be completely sustainable [66]. For these reasons, we did not consider the fuel production as a relevant factor in the environmental impact.

Finally, the space industry manufacturing environmental impact is usually not taken into account given the limited number of units that are produced each year. Nonetheless, if this project was carried out, it would reach numbers comparable to the car industry. Assuming that the sailcraft were manufactured during a 20 year time period, around 75 million vehicles would need to be produced per year. In 2017 the European Union produced 17 million cars, with around 9.5 million tonnes of CO_2 emitted in the process [67]. Given the similarity in the numbers, it was considered that these two industries could be compared, but a car weights around one ton, whereas the spacecraft considered has a mass of 55 kg. Taking this into consideration, it seemed reasonable to assume that the emissions of manufacturing the sailcraft would be around three times smaller than the value previously mentioned, giving a total of around 3 million tonnes of CO_2 per year, thus insignificant compared to the launches.

8.6. Cost of the system compared to cost of climate change to society

The total cost of the proposed sunshade system to control global temperature increase is mainly driven by the launch. Elon Musk is not the only one expecting a launch cost of "tens of dollar per kilogram" by 2040, see e.g. Ref. [68] where this quote from NASA is given. The estimate we make of US$50/kg is very likely within a factor of two of what it actually will be and it could well become as low as US$20-30/kg. On the other hand, the development of the solar sail technology might not reach as far as we have assumed and the total mass to launch might increase considerably. It is therefore wise to give a total cost range of 5–10 trillion dollar for a system that could avoid a global temperature increase of 1 °C. If 2 °C is needed, the cost will be more or less double. Further studies should give a better estimate of both the cost for a given size of a sunshade system and the required size.

In any case, the cost must be put in perspective: If not sufficient actions are taken, what is the global damage of the corresponding temperature increase? It is arguably very hard to predict the cost of temperature increase and there is a large spread of estimates for this number. In one study from 2018, Burke et al. wrote "we project 15%–25% reductions in per capita output by 2100 for the 2.5–3 °C of global warming implied by current national commitments" [69]. The world Global Domestic Product (GDP) today is around US$100 trillion per year and will continue to grow. Leimbach et al. predicted a global GDP ranging between US$309 trillion and US$906 trillion by 2100 [70].

Thus, the loss caused by a temperature increase of 3 °C above pre-industrial levels would range between US$46 and US$77 trillion for the most pessimistic GDP forecast, and between US$136 and US$227 for the most optimistic one. On the other hand, other studies have suggested lower climate damage costs, e.g Nordhaus in 2018 estimated 2% of GDP, although stressing that there are large uncertainties [6]. To turn it around, the sunshade system corresponds to an investment of about US $300 billion per year, if the cost is spread over 25 years, say 2035–2060. That is a few per mille of the world GDP in that time frame. After that, for as long as the CO_2 remains in the atmosphere, the cost of maintaining the system is much less, while the benefits for the global economy remains the same. If the damage to global economy and society is more than a few times 0.1% of global GDP, it would clearly be economically advantageous to deploy a sunshade system.

9. Conclusion

The implementation of space based geoengineering techniques has rarely been studied from a practical point of view. This paper aims to shed some light to the feasibility of this practical realization in the near future, offering a first approximation on how it could be achieved, the advancements necessary to do so and the costs.

It has been argued that in about 15 years, given the resources, the technology of solar sailing could be advanced to the level that a sailcraft with an area of up to 9000 m^2 could be built, with the capacity to sail from a LEO of 2000 km altitude to the vicinity of the Lagrange point L_1 between Earth and the Sun. These sails could be used as sunshades to compensate for global temperature increase. To obtain a 1 °C temperature reduction, around 1.5 billion sailcraft would be needed, with a total system mass of 8.3×10^{10} kg. The total cost of manufacturing and launching the whole system is estimated to be in the range of US$5–10 trillion, based on projections on future launch vehicles. If sail membrane technology can be developed to allow coating with very low reflectivity and low emissivity, these numbers could be reduced considerably. The cost is in the order of 0.1% of the world GDP during the twenty years it is proposed to deploy the system. This is very likely much less than the cost of the possible damages due to an excessive temperature rise. Still, a decision to produce the whole system should not be taken before, and only if, it is certain that a global temperature rise above 2 °C cannot be avoided. However, the technological development to reach at least TRL 7 within 15 years should be started immediately.

In addition to increasing the TRL for solar sailing, the large numbers of spacecraft and launches of the system represent the main challenge for the project to become a reality. Production lines of scales never seen before in the space industry have to be set up. In any case, the next step towards the development of a full system is a fairly simple and straightforward one: make a demonstrator sailcraft of modest size (e.g. 10 m × 10 m) and show that it can solar sail from Earth orbit to L_1.

Declaration of competing interest

The authors declare that they have no known competing financial interests or personal relationships that could have appeared to influence the work reported in this paper.

References

[1] V. Masson-Delmotte, P. Zhai, H.-O. Pörtner, D. Roberts, J. Skea, P. Shukla, et al., Summary for policymakers, in: Global Warming of 1.5◦C. An IPCC Special Report on the Impacts of Global Warming of 1.5◦C above Pre-industrial Levels and Related Global Greenhouse Gas Emission Pathways, in the Context of Strengthening the Global Response to the Threat of Climate Change, Sustainable Development, and Efforts to Eradicate Poverty, Tech. rep., IPCC, 2018.
[2] J. Blunden, D. Arndt, State of the climate in 2019, Bull. Am. Meteorol. Soc. 101 (8) (2020), https://doi.org/10.1175/2020BAMSStateoftheClimate.1.
[3] M.C. Hänsel, M.A. Drupp, J.A. J D, F. Nesje, C. Azar, M.C. Freeman, B. Groom, T. Sterner, Climate economics support for the un climate, Nat. Clim. Change 10 (2020) 781–789, https://doi.org/10.1038/s41558-020-0833-x.
[4] J. Hassler, P. Krusell, C. Olovsson, The consequences of uncertainty: climate sensitivity and economic sensitivity to the climate, Annual Review of Economics 10 (2018) 189–205, https://doi.org/10.1146/annurev-economics-080217-053229.
[5] U N E Programme, Emissions Gap Report 2019, Tech. rep., UNEP, 2019.
[6] W. Nordhaus, Projections and uncertainties about climate change in an era of minimal climate policies, American Economic Journal: Economic Policy 2018 10 (3) (2018) 333–360, https://doi.org/10.1257/pol.20170046.
[7] P. Irvine, B. Kravitz, M. Lawrence, H. Muri, An overview of the Earth system science of solar geoengineering, WIREs Clim Change 7 (6) (2016) 815–833, https://doi.org/10.1002/wcc.423.

[8] S. Maruyama, Concept design of linear-motor-accelerated projectile for nanoparticle dispersion in stratosphere, Thermal Science and Engineering Progress 15 (2020) 100437, https://doi.org/10.1016/j.tsep.2019.100437.
[9] W. Seifritz, Mirrors to halt global warming? Nature 340 (1989) 603, https://doi.org/10.1038/340603a0.
[10] J. Early, Space-based solar shield to offset greenhouse effect, J. Br. Interplanet. Soc. (JBIS) 42 (1989) 567–569.
[11] M. Mautner, K. Parks, Space-based control of the climate, Engineering, Construction, and Operations in Space II (1990) 1159–1168.
[12] H. Hudson, A space parasol as a countermeasure against the greenhouse effect, J. Br. Interplanet. Soc. (JBIS) 44 (1991) 139–144.
[13] E. Teller, L. Wood, R. Hyde, Global Warming and Ice Ages: I. Prospects for Physics Based Modulation of Global Change, 1996.
[14] R. Angel, Feasibility of cooling the earth with a cloud of small spacecraft near the inner Lagrange point (L1), Proceedings of The National Academy of Sciences of the USA 103 (46) (2006) 17184–17189, https://doi.org/10.1073/pnas.0608163103.
[15] C. McInnes, Minimum mass solar shield for terrestrial climate control, J. Br. Interplanet. Soc. (JBIS) 55 (2002) 307–311.
[16] J.-P. Sánchez, C. McInnes, Optimal sunshade configurations for space-based geoengineering near the sun-earth L1 point., PloS One 10 (8). doi:10.1371/journal.pone.0136648.
[17] A. Jehle, E. Scott, R. Centers, A Planetary Sunshade Built From Space Resources (2020), https://doi.org/10.2514/6.2020-4077.
[18] T. Kosugi, Role of sunshades in space as a climate control option, Acta Astronaut. 67 (1) (2010) 241–253, https://doi.org/10.1016/j.actaastro.2010.02.009.
[19] D. Spencer, L. Johnson, A. Long, Solar sailing technology challenges, Aero. Sci. Technol. 93 (2019) 105276, https://doi.org/10.1016/j.ast.2019.07.009.
[20] B. Govindasamy, K. Caldeira, Geoengineering Earth's radiation balance to mitigate CO2-induced climate change, Geophys. Res. Lett. 27 (14) (2000) 2141–2144, https://doi.org/10.1029/1999GL006086.
[21] G. Bala, P.B. Duffy, K.E. Taylor, Impact of geoengineering schemes on the global hydrological cycle, Proc. Natl. Acad. Sci. Unit. States Am. 105 (22) (2008) 7664–7669, https://doi.org/10.1073/pnas.0711648105.
[22] C. McInnes, Solar Sailing. Technology, Dynamics and Mission Applications, Springer-Verlag, 1999.
[23] C. McInnes, Planetary macro-engineering using orbiting solar reflectors, Macro-engineering: a challenge for the future (2006) 215, https://doi.org/10.1007/1-4020-4604-9_11.
[24] C. McInnes, Space-based geoengineering: challenges and requirements, Proc. IME C J. Mech. Eng. Sci. 224 (3) (2010) 571–580, https://doi.org/10.1243/09544062JMES1439.
[25] A. Farrag, T. Mahmoud, A. ElRaffiei, Satellite swarm survey and new conceptual design for earth observation applications, The Egyptian Journal of Remote Sensing and Space Sciencesdoi:10.1016/j.ejrs.2019.12.003.
[26] Y. Tsuda, O. Mori, R. Funase, H. Sawada, T. Yamamoto, T. Saiki, et al., Achievement of IKAROS — Japanese deep space solar sail demonstration mission, Acta Astronaut. 82 (2) (2013) 183–188, https://doi.org/10.1016/j.actaastro.2012.03.032.
[27] Y. Tsuda, O. Mori, R. Funase, H. Sawada, T. Yamamoto, T. Saiki, et al., Flight status of IKAROS deep space solar sail demonstrator, Acta Astronaut. 69 (9) (2011) 833–840, https://doi.org/10.1016/j.actaastro.2011.06.005.
[28] J. Mansell, D.A. Spencer, B. Plante, A. Diaz, M. Fernandez, J. Bellardo, B. Betts, B. Nye, Orbit and attitude performance of the LightSail 2 solar sail spacecraft, in: AIAA Scitech 2020 Forum, 2020, https://doi.org/10.2514/6.2020-2177. https://arc.aiaa.org/doi/abs/10.2514/6.2020-2177.
[29] T. P. Society, Light sail. fly by light for cubesats, https://www.planetary.org/sci-tech/lightsail, accessed: 2020-18-11.
[30] J.P. Eastwood, D.O. Kataria, C.R. McInnes, N.C. Barnes, P. Mulligan, Sunjammer, Weather 70 (1) (2015) 27–30, https://doi.org/10.1002/wea.2438.
[31] R. Young, Updated Hdeliostorm Warning Mission: Enhancements Based on New Technology, Tech. Rep, NASA Marshall Space Flight Center, 2006.
[32] WPTherml, https://foleylab.github.io/wptherml/, accessed: 2021-02-05.
[33] P. Hager, Thermal design and verification, in: Fly Your Satellite! 3 Selection Workshop, ESA ESTEC - TEC-MTT Thermal Control Section, ESTEC, Noordwijk, The Netherlands, 2019.
[34] S. Gong, M. Macdonald, Review on solar sail technology, Astrodynamics 3 (2) (2019) 93–125, https://doi.org/10.1007/s42064-019-0038-x.
[35] B. Derbes, G. Veal, J. Rogan, C. Chafer, Team encounter solar sails, in: 45th AIAA/ASME/ASCE/AHS/ASC Structures, Structural Dynamics & Materials Conference, 2004, https://doi.org/10.2514/6.2004-1577.
[36] C. McInnes, M. Eiden, P. Groepper, T. Peacock, Solar sailing – mission opportunities and innovative technology demonstration, in: Tech. Rep. Bulletin, vol. 108, ESA, 2001.
[37] O. Eldad, E. Lightsey, Attitude control of the sunjammer solar sail mission, in: Proceedings of the AIAA/USU Conference on Small Satellites, AIAA/Utah State Univ, Logan, Utah, 2014. http://digitalcommons.usu.edu/smallsat/2014/Propulsion/3.
[38] N. Systems, NewSpace systems: ADCS solutions. https://www.newspacesystems.com/, 2020. (Accessed 15 November 2020).
[39] RUAG, Electronics RUAG. https://www.ruag.com/en/products-services/space/electronics, 2020. (Accessed 15 November 2020).
[40] O. De Weck, A systems approach to mass budget management, 11th AIAA/ISSMO Multidisciplinary Analysis and Optimization Conferencedoi:10.2514/6.2006-7055.
[41] R. Young, E. Montgomery, C. Adams, TRL assessment of solar sail technology development following the 20-meter system ground demonstrator hardware testing, 2007, https://doi.org/10.2514/6.2007-2248.
[42] J. Grundmann, W. Bauer, J. Biele, R. Boden, M. Ceriotti, F. Cordero, et al., Capabilities of Gossamer-1 derived small spacecraft solar sails carrying Mascot-derived nanolanders for in-situ surveying of NEAs, Acta Astronaut. 156 (2019) 330–362, https://doi.org/10.1016/j.actaastro.2018.03.019. http://www.sciencedirect.com/science/article/pii/S009457651731398X.
[43] M. Peck, J. Atchison, Length scaling in spacecraft dynamics, J. Guid. Contr. Dynam. 34 (1) (2011) 231–246, https://doi.org/10.2514/1.49383.
[44] SpaceX, Starlink. https://www.starlink.com/, 2020. (Accessed 24 November 2020).
[45] OneWeb, OneWeb. https://www.oneweb.world/, 2020. (Accessed 24 November 2020).
[46] V. Coverstone, J. Prussing, Technique for escape from geosynchronous transfer orbit using a solar sail, J. Guid. Contr. Dynam. 26 (4) (2003) 628–634, https://doi.org/10.2514/2.5091.
[47] M. Otten, C. McInnes, Near minimum-time trajectories for solar sails, J. Guid. Contr. Dynam. 24 (3). doi:10.2514/2.4758.
[48] P. Gill, E. Wong, User's Guide for SNOPT-MATLAB:Matlab Interface for Nonlinear Optimizer SNOPT, University of California, La Jolla, CA 92093-0112, USA, April 2017.
[49] J. Bookless, C. McInnes, Control of Lagrange point orbits using solar sail propulsion, Acta Astronaut. 62 (2) (2008) 159–176, https://doi.org/10.1016/j.actaastro.2006.12.051.
[50] Space Exploration Technologies Corp., Starship User's Guide (March 2020).
[51] F.A. Administration, Air traffic by the numbers. https://www.faa.gov/air_traffic/by_the_numbers/, 2020. (Accessed 25 November 2020).
[52] SpaceX, Falcon heavy capabilities. https://www.spacex.com/media/Capabilities&Services.pdf. (Accessed 9 October 2020).
[53] M. Wall, SpaceX's Starship May Fly for Just $2 Million Per Mission, Elon Musk Says, 2019. https://www.space.com/spacex-starship-flight-passenger-cost-elon-musk.html. (Accessed 21 October 2020).
[54] SpaceX, Application for fixed satellite service by space exploration holdings, llc, Tech. Rep. SAT-LOA-20170301-00027 (03 2017).
[55] A. Buis, The atmosphere: getting a handle on carbon dioxide, in: Sizing up Humanity's Impacts on Earth's Changing Atmosphere: A Five-Part Series. Part 2, 2019. https://climate.nasa.gov/news/2915/the-atmosphere-getting-a-handle-on-carbon-dioxide/. (Accessed 25 November 2020).
[56] Voyager - Mission Status , https://voyager.jpl.nasa.gov/mission/status/, accessed: 2020-11-23.
[57] N. Melnik, U. Geppert, B. Biering, F. Lura, Light pressure measurement at DLR Bremen, Advances in Solar Sailing (2014) 399–406, https://doi.org/10.1007/978-3-642-34907-2.
[58] Enpulsion, Enpulsion Micro R3, 2021.
[59] C.R. McInnes, Solar sail mission applications for non-keplerian orbits, Acta Astronaut. 45 (4) (1999) 567–575, https://doi.org/10.1016/S0094-5765(99)00177-0, third IAA International Conference on Low-Cost Planetary Missions.
[60] M. Macdonald, C. McInnes, Solar sail science mission applications and advancement, Adv. Space Res. 48 (11) (2011) 1702–1716, https://doi.org/10.1016/j.asr.2011.03.018.
[61] D. Lunt, A. Ridgwell, P. Valdes, A. Seale, "Sunshade World": a fully coupled GCM evaluation of the climatic impacts of geoengineering, Geophys. Res. Lett. 35 (12). doi:10.1029/2008GL033674.
[62] D. MacMartin, D. Keith, B. Kravitz, K. Caldeira, Management of trade-offs in geoengineering through optimal choice of non-uniform radiative forcing, Nat. Clim. Change 3 (2013) 365–368, https://doi.org/10.1038/nclimate1722.
[63] B. Graver, D. Rutherford, S. Zheng, co_2 emissions from commercial aviation, in: 2018, and 2019, Tech. Rep. SAT-LOA-20170301-00027, The International Council on Clean Transportation (10 2020, 2013.
[64] IEA, Tracking transport 2020. https://www.iea.org/reports/tracking-transport-2020, 2020.
[65] X. Lan, B. Hall, G. Dutton, J. Muhl, J. Elkins, Atmospheric composition (in state of the climate in 2019, chapter 2: Global climate), Special Online Supplement to the Bulletin of the American Meteorological Society 101 (8). doi:10.1175/BAMS-D-20-0104.1.
[66] J.P. Stempien, M. Ni, Q. Sun, S.H. Chan, Production of sustainable methane from renewable energy and captured carbon dioxide with the use of Solid Oxide Electrolyzer: a thermodynamic assessment, Energy 82 (2015) 714–721, https://doi.org/10.1016/j.energy.2015.01.081.
[67] ACEA, Environmental Impact of Car Production Strongly Reduced over Last Decade, Press release, 2018. https://www.acea.be/press-releases/article/environmental-impact-of-car-production-strongly-reduced-over-last-decade. (Accessed 16 November 2020).
[68] NASA, Advanced space transportation program: paving the highway to space. https://www.nasa.gov/centers/marshall/news/background/facts/astp.html, 2008. (Accessed 29 October 2020).
[69] M. Burke, W. Davis, D. N S, Large potential reduction in economic damages under UN mitigation targets, Nature 557 (2018) 549–553, https://doi.org/10.1038/s41586-018-0071-9.
[70] M. Leimbach, E. Kriegler, N. Roming, J. Schwanitz, Future growth patterns of world regions – a GDP scenario approach, Global Environ. Change 42 (2017) 215–225, https://doi.org/10.1016/j.gloenvcha.2015.02.005.